UCRL 736
Copy 2

UNIVERSITY OF CALIFORNIA
Ernest O. Lawrence
Radiation Laboratory

TWO-WEEK LOAN COPY

This is a Library Circulating Copy which may be borrowed for two weeks. For a personal retention copy, call Tech. Info. Division, Ext. 5545

BERKELEY, CALIFORNIA

DISCLAIMER

This document was prepared as an account of work sponsored by the United States Government. While this document is believed to contain correct information, neither the United States Government nor any agency thereof, nor the Regents of the University of California, nor any of their employees, makes any warranty, express or implied, or assumes any legal responsibility for the accuracy, completeness, or usefulness of any information, apparatus, product, or process disclosed, or represents that its use would not infringe privately owned rights. Reference herein to any specific commercial product, process, or service by its trade name, trademark, manufacturer, or otherwise, does not necessarily constitute or imply its endorsement, recommendation, or favoring by the United States Government or any agency thereof, or the Regents of the University of California. The views and opinions of authors expressed herein do not necessarily state or reflect those of the United States Government or any agency thereof or the Regents of the University of California.

UNCLASSIFIED

UCRL-736

May 31, 1950

cy 2.

Variation of High Energy Neutron Collision Cross Sections of Nuclei with Energy

By

James DeJuren

A.B. (University of California) 1940

DISSERTATION

Submitted in partial satisfaction of the requirements for the degree of

DOCTOR OF PHILOSOPHY

in

Physics

in the

GRADUATE DIVISION

of the

UNIVERSITY OF CALIFORNIA

Approved:

. . . . . .

. . . . . .

. . . . . .

Committee in Charge

Deposited in the University Library . . . . . .

Date Librarian

TABLE OF CONTENTS

Page

LIST OF TABLES

LIST OF ILLUSTRATIONS

Section 1 Introduction 1

Section II Counters and Neutron Detection 6

Section III Experimental Arrangement 10

Section IV Attenuator Materials 13

Section V Sources of Error 14

Section VI Results 18

Section VII Discussion of Results 20

Acknowledgements 23

References 24

LIST OF TABLES

		Page
Table 1	Differential Scattering Cross Sections	16
Table 2	Total Cross Sections of Nuclei for High Energy Neutrons Measured with Bismuth Fission Chambers	19
Table 3	Total Cross Sections for 95 and 270 Mev. Neutrons Measured Previously with Bismuth Fission Chambers	19a

LIST OF ILLUSTRATIONS

Figure 1	Internal structure of bismuth fission chamber	Section II
Figure 2	Discriminator curve of bismuth fission chamber	Section II
Figure 3	Plan view of experimental arrangement	Section III
Figure 4	Graph of total neutron cross sections versus energy of carbon, aluminum, copper, and lead	Section VI
Figures 5 and 6	Graphs of total n-p cross section as function of neutron energy	Section VI

VARIATION OF HIGH ENERGY NEUTRON COLLISION CROSS SECTIONS OF NUCLEI WITH ENERGY

James DeJuren

I. INTRODUCTION

The development of particle accelerators has permitted the production of high energy neutrons by various bombardment reactions. For the high energies obtained the width of nuclear energy levels is much greater than the level spacing and the resonance effects noted in the cross section measurements for lower energy neutrons disappear. Measurements by Amaldi[1] et al with 14 Mev. neutrons and by Sherr[2] with 25 Mev. neutrons were interpreted in the light of an opaque nuclear model for which the total cross section is $\sigma_t = 2\pi R_c^2$

where R_c is called the collision radius.

If an opaque nucleus intercepts a plane neutron wave, the removal of a disc of radius R_c from the wave will result in an equal loss from the remaining wave by "diffraction scattering". The total cross section will be twice the inelastic cross section. If the opaque nucleus is assumed to be a sphere with the same density of nuclear matter for all nuclei, the collision radius is

$$R_c = b + r_o A^{1/3}$$

where b is variously interpreted as the range of nuclear forces or the wave length $\lambda\!\!\!^{-}$ of the incident neutron. Graphically b is the intercept obtained when R_c is plotted against $A^{1/3}$. From an analysis of the 14 - 25 Mev. cross section data McMillan deduced the value $r_o = 1.37 \times 10^{-13}$ cm.

Nuclear collision cross sections for high energy neutrons are usually analyzed by the expansion of a plane (neutron) wave into a series of spherical

harmonics:

$$e^{ikz} = e^{ikr\cos\theta} = \sum_{l=0}^{\infty} (2l+1) i^l P_l(\cos\theta) f_l(r)$$

where $f_l(r) = \left(\frac{\pi}{2kr}\right)^{1/2} J_{l+\frac{1}{2}}(kr)$

$J_{l+\frac{1}{2}}(kr)$ is the Bessel function of order $l+\frac{1}{2}$ and at large r the asymptotic expension of $f_l(r)$ is

$$f_l(r) \sim \frac{\sin(kr - \frac{l\pi}{2})}{kr} = \frac{e^{i(kr - \frac{l\pi}{2})} - e^{-i(kr - \frac{l\pi}{2})}}{2ikr}$$

The values of l correspond to the allowed integral multiples of $\hbar$ that the neutron angular momentum may assume with respect to the center of the nucleus (which is assumed to be massive). Writing $f_l(r)$ in exponential form the first term corresponds to an outgoing and the second to an incoming spherical wave. If the plane wave impinges upon a nucleus the amplitude of an outgoing partial spherical wave may be diminished by a factor η_l corresponding to absorption and the phase may be altered by a shift $2\delta_l$. The radial function becomes

$$F_l(r) = \eta_l \frac{e^{2i\delta_l} e^{i(kr - \frac{l\pi}{2})} - e^{-i(kr - \frac{l\pi}{2})}}{2ikr}$$

where $\eta_l \leq 1$

Then

$$\psi = (2l+1) i^l P_l(\cos\theta) \left[\eta_l \frac{e^{2i\delta_l} e^{i(kr - \frac{l\pi}{2})} - e^{-i(kr - \frac{l\pi}{2})}}{2ikr} \right]$$

represents the wave function resulting from the interaction of the neutron wave and the nucleus; and

$$u = \psi - e^{ikz} = \sum_l (2l+1) i^l P_l(\cos\theta) \left[\frac{(\eta_l e^{2i\delta_l} - 1) e^{i(kr - \frac{l\pi}{2})}}{2ikr} \right]$$

is therefore the scattered wave.

The elastic scattering cross section is obtained by calculating the flux $\int |u|^2 v \, d\tau$ over a large sphere (v is the velocity of the neutrons $= \frac{\hbar k}{m}$). The scattered flux divided by the incoming flux/cm^2 which is equal is the elastic scattering cross section. The absorption cross section is found similarly by the differences of the

incoming and outgoing currents of the two waves implicit in ψ. Writing $\psi = \psi_o + \psi_i$ (for outgoing and incoming waves)

$$\sigma_a = \sigma_{inelastic} = \sum_{\ell=0}^{\infty} \int [v|\psi_i|^2 - v|\psi_o|^2]\, d\tau$$

$$= \sum_{\ell=0}^{\infty} (2\ell+1)(1-\eta_\ell^2)\pi \lambda\!\!\!^{-2}$$

and $$\sigma_e = \sum_{\ell=0}^{\infty} [(1-\eta_\ell)^2 + 4\eta_\ell \sin^2\delta_\ell](2\ell+1)\pi \lambda\!\!\!^{-2}$$

For high energies the maximum ℓ is given by $pR = \ell_{max.}\hbar$ or $\ell_m = \frac{R}{\lambda\!\!\!^{-}}$ where R is the radius of the nucleus. For the special case of an opaque nucleus $\eta_\ell = 0$ for $\ell < \ell_{max.}$ and $\begin{cases}\delta_\ell = 0 \\ \eta_\ell = 1\end{cases}$ for $\ell > \ell_m$

Then $$\sigma_t = \sigma_e + \sigma_a = 2\sum_{\ell=0}^{\ell_{max.}} (2\ell+1)\pi \lambda\!\!\!^{-2}$$

$$= (\ell_m + 1)^2 \pi \lambda\!\!\!^{-2}$$

$$= 2\pi(R + \lambda\!\!\!^{-})^2$$

Our assumptions are only valid if $R > \lambda\!\!\!^{-}$ so

$\sigma_t \sim 2\pi R^2$ or the total cross section is twice the geometric cross section.

For a nucleus partially transparent η_ℓ will not be zero for $\ell \lambda\!\!\!^{-} < R$ and will vary with ℓ, since the path length of a partial wave in nuclear matter is a function of ℓ. This variation of η_ℓ is taken into account in the theory of the transparent nucleus discussed later. Weisskopf[3] discusses the above material in greater detail.

The production of neutrons with a mean energy of 90 Mev. from the stripping of 190 Mev. deuterons by a 0.5" Be target in the 184" cyclotron[4] made it possible to extend the measurements to a region in which the scattering mean free path of a neutron traversing nuclear matter was expected to be comparable to the nuclear radius. At these energies, therefore, the nuclei should appear partially transparent to the bombarding neutrons.

Experiments were performed by Cook, McMillan, Peterson, and Sewell[5] using the 20.5 minute half life beta activity resulting from $C^{12}(n,2n)C^{11}$ for detection and by DeJuren and Knable[6] employing bismuth fission for detection. The two sets of measurements have estimated mean neutron detection energies of 84 and 95 Mev. respectively. Both experiments exhibited marked transparency effects, especially for light nuclei, and the 95 Mev. cross section values were roughly 10% less than the 84 Mev. results.

Fernbach, Serber, and Taylor[7] have developed a model of the transparent nucleus, in which the nucleus is regarded as a sphere of nuclear matter of uniform density characterized by an absorption coefficient, K, and an index of refraction due to the increase of the neutron propagation vector, k, when the neutron wave enters the nucleus. If the propagation vector outside the nucleus is $k = \frac{(2ME)^{1/2}}{\hbar}$, the increase in the propagation vector $k_1 = k\left[\left(1+\frac{V}{E}\right)^{1/2} - 1\right]$, where V is the potential depth of the nuclear well. A wave going a distance X in nuclear matter will have its amplitude and relative phase modified by a factor $a = e^{\left(-\frac{1}{2}K + i k_1 X\right)}$. The difference in amplitude of the wave emerging from the sphere and the unobstructed wave represents a diffracted wave and leads to the diffraction or elastic scattering cross section. The solutions for the inelastic and elastic cross sections are respectively

$$\sigma_i = \pi R^2 \left\{ 1 - \frac{1-(1+2KR)e^{-2KR}}{2K^2R^2} \right\}$$

$$\sigma_e = 2\pi \int_0^R \left| 1 - e^{(-K + 2ik_1 s)} \right|^2 s\,ds$$

$$\sigma_t = \sigma_i + \sigma_e$$

The result for σ_e is merely indicated to avoid the complex integrated expression.

The constants k_1 and K are chosen to give the best straight line fit for the radius, R, calculated with these expressions from the total cross section data, plotted against $A^{1/3}$. For both the 84 and 95 Mev. data $R = 1.38\ A^{1/3} \times 10^{-13}$ cm. is the line of best fit. The radius line becomes appreciably curved if k_1 is varied by 5% from its optimum value, but K can be varied by 25% before the curvature is noticeable. Since the inelastic cross sections, using this model, are a function of K and R alone the inelastic cross sections measured at 95 Mev. define K more accurately than the total cross section measurements. For the 95 Mev. data $k_1 = 2.85 \times 10^{+12}\ cm^{-1}$ and $K = 3.0 \times 10^{+12}\ cm^{-1}$ were the values providing the best fit for the model.

The production of neutrons with a mean energy of 270 Mev. by bombardment of a 2" Be target with 350 Mev. neutrons provided a further extension of the energy dependence of the cross sections. Measurements by Fox, Leith, Wouters and McKenzie[8] with scintillation counters and by DeJuren[9] with bismuth fission chambers yielded total cross section values that agreed well with each other. To obtain even an approximate fit of the data with the transparent model, it was necessary to let $k_1 = 0$, inferring that at these energies the neutron apparently experiences no potential change upon entering a nucleus. The ratios of inelastic to total cross section for carbon, copper, and lead were measured with bismuth fission chambers and were equal to 0.5 within the statistical errors. Since the bismuth fission threshold is much less than the mean neutron energy of 270 Mev. the results can only be safely interpreted as the lower limit of the ratio of $\frac{\sigma_i}{\sigma_t}$.

As the energy interval between the 95 and 270 Mev. measurements was

wide and the agreement of the model of the transparent nucleus with the experimental data at 270 Mev. was unsatisfactory, it was felt necessary to investigate the variation of neutron total cross sections of a representative number of nuclei within this energy region.

II. COUNTERS AND NEUTRON DETECTION

A. Counters

The bismuth fission ionization chambers[10] employed in the present measurements were previously used in the 95 and 270 Mev. total cross section measurements. The chambers contain 31 aluminum discs 1/32 inches thick and 2 inches in diameter (Figure 1). Alternate discs are coated on both sides with thin layers of bismuth and connected in parallel. The uncoated discs, connected in parallel, collect the electrons formed by ionization of the fission fragments. The discs are mounted 3/8 inches apart and the capacity of the system is of the order of 100$\mu\mu f$. A field strength of 500 to 600 v/cm. is maintained between the sets of plates. A heavy fragment produced by the fission of a bismuth nucleus is initially multiply charged and ionizes most heavily at the beginning of its range. As its velocity decreases orbital electrons are captured and the number of ion pairs formed per cm. decreases. Hence most of the ionization in the gas occurs near the negative bismuth-coated plates and the size of the resulting pulse will be approximately proportional to the energy of the fission fragment. The pulses are suitably amplified by linear amplifiers.

B. Pulse Characteristics

The number of ions produced by a bismuth fission fragment is much greater than that produced by an alpha particle or proton given off by a spallation reaction in the chamber. Consequently it will take coincidences of several alphas (and protons) to give a pulse as large as a fission pulse. If at a given neutron intensity the logarithm of the chamber counting rate relative to a fixed monitor is plotted against the discriminator voltage a curve with

a broad plateau is obtained (Figure 2). If the neutron intensity is increased, the rapidly varying "pileup" region is shifted to the right to higher discriminator settings, but the remainder of the curve is unchanged in shape. For multiple coincidences the rapid increase in counting rate with change in neutron intensity is expected and affords a criterion for distinguishing fission pulses from "pileups". To select the operating discriminator voltage, the linear portion of the "pileup" curve is extrapolated below the plateau region and a point on the plateau is selected where the fission pulse counting rate is a factor of 500 or more greater than the multiple coincidence rate. This selection is made at the highest neutron intensity to be used during the measurements and any reduction in the intensity will further depress the ratio of "pileups" to fission pulses.

The gas used, 95% argon and 5% CO_2, was maintained at a pressure of half an atmosphere. At this pressure 90 Mev. fission fragments have a range equal approximately to the plate separation in the chamber. Since the ionization from the initially multiply charged fission fragments occurs near the negative bismuth coated discs, increasing the pressure will not increase the size of the fission pulses; however, alphas and protons which have ranges greater than the plate separation will give pulses that increase almost linearly with pressure. Therefore fewer coincidences of alphas and protons are needed to give a pulse as large as a fission pulse at the higher pressure. This effect has been verified experimentally with the chambers. At one-half atmosphere and at a fission counting rate of 10 per second from the neutron beam satisfactory plateaus with negligible "pileup" contributions at the operating discriminator voltage were always obtained.

C. Effective Neutron Detection Energy

The energy distribution of the neutrons knocked out of the 2" Be target by the 350 Mev. protons has been measured by Hadley[11], by Fox, Leith and Wouters[12] and by Kelly and Wiegand[13]. All three measurements show a distribution peaked around 270 Mev. with a width at half maximum of about 60 Mev. The statistical errors are rather high and Hadley and Cladis are attempting to measure the distribution from a 0.5" Be target with more precision. To investigate the variation of the bismuth fission cross section with neutron energy two types of measurements were made. First the ratio of the bismuth fission cross section to the n,2n cross section of carbon for the 270 Mev. neutrons relative to the ratio for the 90 Mev. neutrons from bombardment of Be by deuterons was measured by placing an 1/8" thick, 1 11/16" diameter polystyrene disc in front of a fission chamber mounted in the collimated neutron flux outside the shielding. The number of fission pulses in the chamber was recorded for steady, 10 minute bombardments and the positron activity resulting from the n,2n reaction of carbon was counted on a standard Geiger-Mueller counter. Bombardments were also made with brass plugs in the collimator to eliminate background effects at both energies. The ratio of the bismuth fission cross section to the n,2n cross section of carbon increased by $3.56 \pm .11$ when the mean neutron energy was raised from 90 to 270 Mev.

Measurements were made inside the shielding of the ratio of the two cross sections by varying the radius of a 0.5" Be target and therefore the energy of the incident protons. A fission chamber and polystyrene disc were placed near the cyclotron tank wall behind 4" of lead, which absorbed stray protons scattered from the target thru the tank wall, but allowed the neutrons to reach the two detectors. The proton energy was lowered by 40 Mev. steps from 350 to 150 Mev. The results

indicated that the ratio of the bismuth fission to the carbon (n,2n) cross section increased almost linearly with the energy of the incident protons, and presumably, therefore, linearly with the mean neutron energy. The carbon (n,2n) cross section is theoretically fairly flat[14] in the energy interval from 90 to 270 Mev., decreasing by a factor of about 0.8. The bismuth fission cross section, therefore, presumably increases in a linear fashion by a factor of three in this energy interval. To obtain a calibration point for the lower proton energies 190 Mev. deuterons were substituted for the protons. The ratio of the bismuth fission to the carbon (n,2n) cross section for the resulting 90 Mev. neutrons was equal to the ratio obtained for the neutrons knocked out by 165 Mev. protons. The mean loss of energy in producing high-energy neutrons in the forward direction by protons appears to be of the order of 75 Mev. for proton energies in the range here employed. A 0.5" Be target (instead of 2") was used in all the measurements to be discussed. Since the proton energy loss in traversing the target is less for the 0.5" than the 2" target and the bismuth fission excitation function is rising by about a factor of three in the neutron energy interval between 90 and 270 Mev., the mean detected neutron energy will be assumed 70 Mev. less than the proton energy. This value is only good to within 10 or 15 Mev., but as the measurements are relative the neutron energy differences will be more accurate. A measurement by Fox and Wouters[15] with scintillation counters of the neutron energy distribution from 180 Mev. protons on a 2" Be target agrees with the above assumption of a constant loss of about 75 Mev. in the neutron energy resulting from proton bombardment.

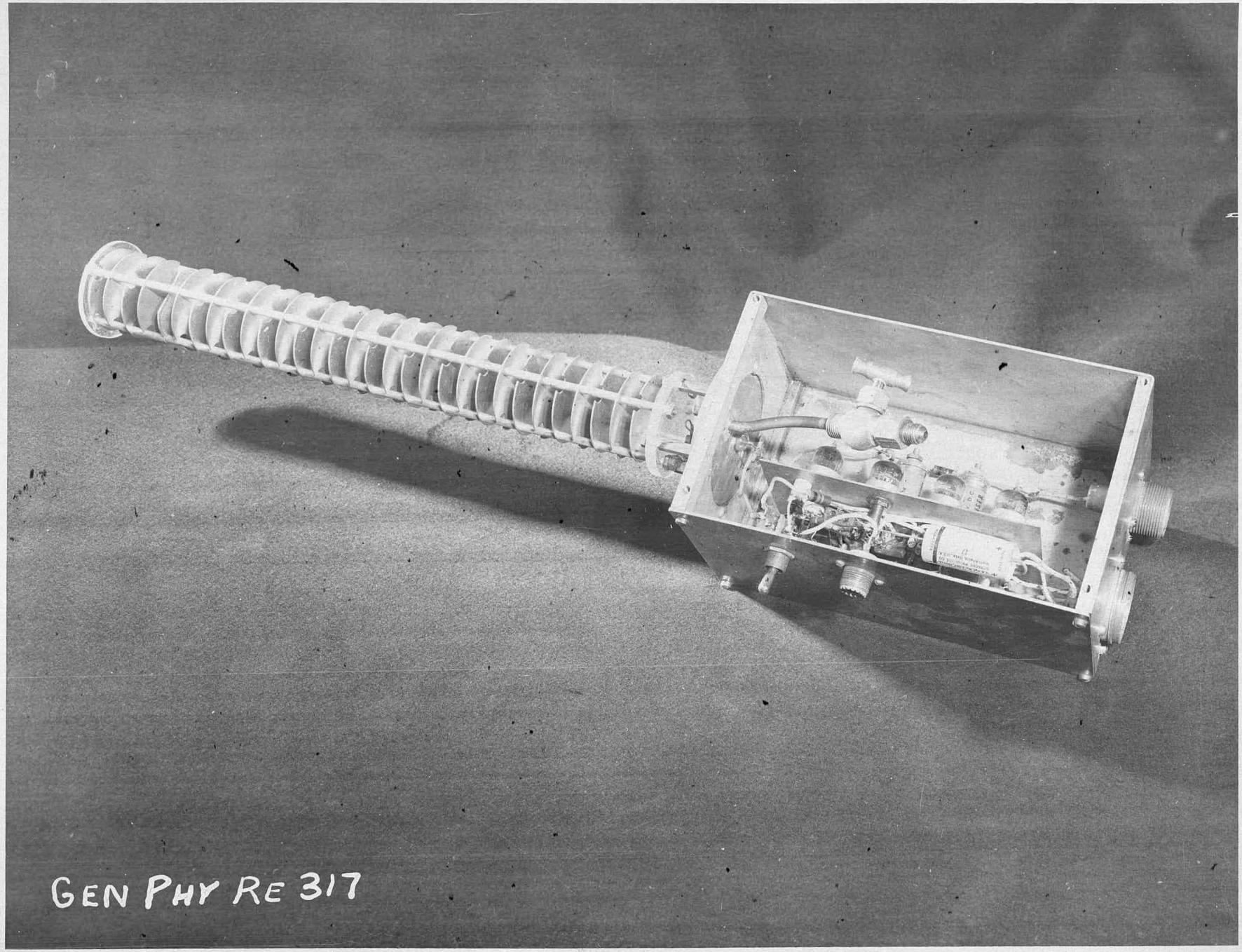

FIG. 1

INTERNAL STRUCTURE OF LONG FISSION IONIZATION CHAMBER

OZ 468

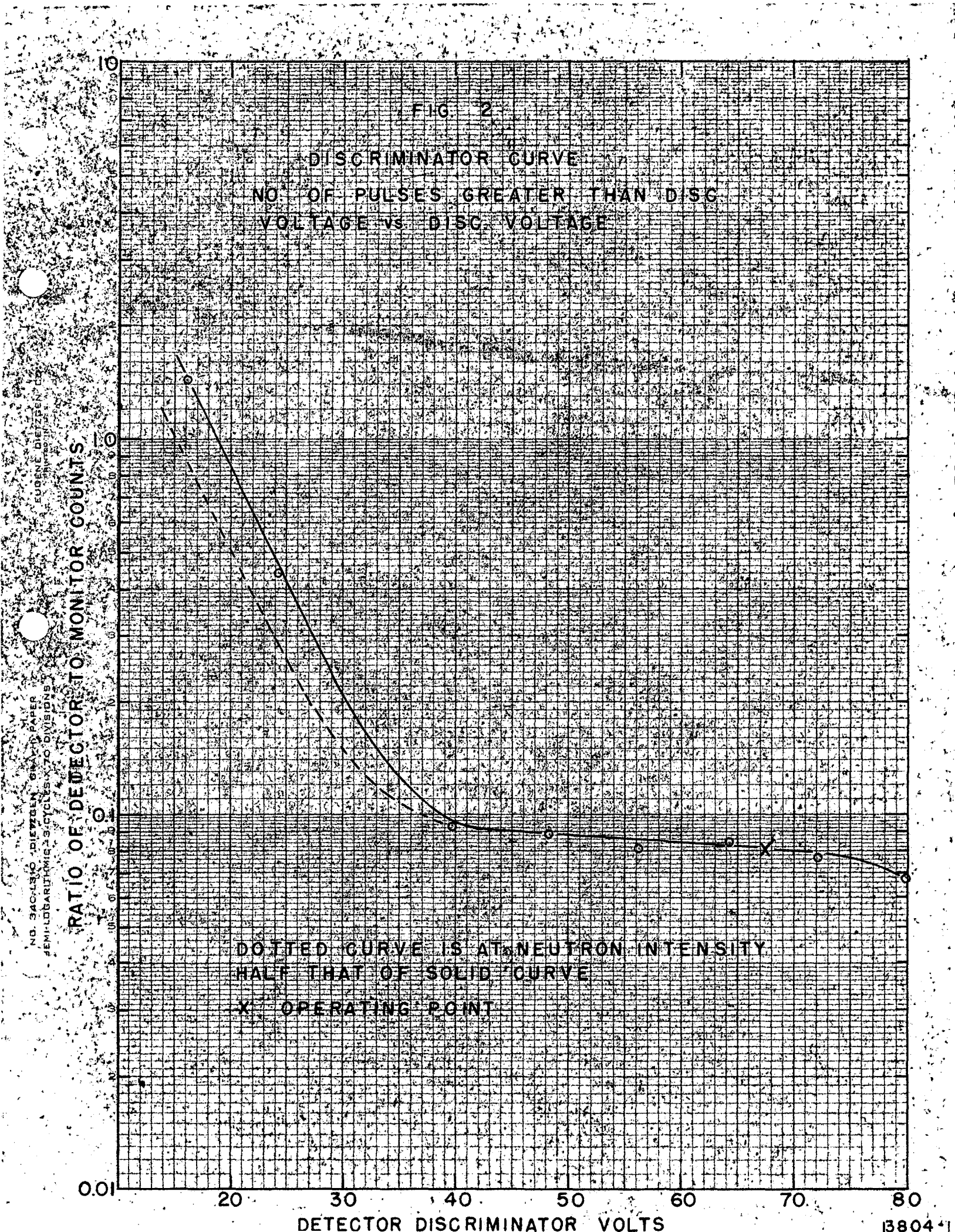
FIG. 2
DISCRIMINATOR CURVE
NO. OF PULSES GREATER THAN DISC. VOLTAGE vs. DISC. VOLTAGE
DOTTED CURVE IS AT NEUTRON INTENSITY HALF THAT OF SOLID CURVE
X OPERATING POINT
RATIO OF DETECTOR TO MONITOR COUNTS
10
1.0
0.1
0.01
20
30
40
50
60
70
80
DETECTOR DISCRIMINATOR VOLTS
13804-1

III. EXPERIMENTAL ARRANGEMENT

The neutrons produced by the bombardment of the 2" Be target by 350 Mev. protons have a wide angular distribution with a half width at half maximum of 25° (as measured with bismuth fission). Since only two collimators are present in the concrete shielding (see Figure 3) corresponding to proton energies of 180 and 350 Mev., the detector must be placed inside the shielding for intermediate energies. Most of the neutron flux passes through an inch of steel tank wall as well as other obstacles; so the elastically scattered flux would constitute a background of perhaps 10 to 20% of the undeviated flux. To reduce the detector background the chamber was placed behind a 7 ft. thick concrete block with a hollow center. Two concrete collimators, each 31" long and 4¼" x 4¼" in area with a 2" diameter opening were placed in series in the center of the concrete block. A brass tube 6' long, 2" outer diameter and 1 13/16" inner diameter was placed inside the concrete collimators for further collimation and to facilitate alignment of target, collimator, and detector. Brass bars, which could be inserted quickly, were packed around the concrete collimators and the rest of the hollow was filled with concrete plugs. The target position was varied from 81" to 54" to obtain the desired proton energy settings and the collimating apparatus could be swivelled into alignment for the target positions. The detector was placed 6' to the rear of the concrete block and the attenuating materials were aligned immediately in front of the block on a wooden holder. The distance from absorbers to detector was about 13', so the geometry was "good" with only small angular scattering corrections necessary.

To monitor the neutron beam a bismuth fission chamber was placed to one side of the concrete block at a position where the contribution of neutrons scattered from the absorbers to its counting rate was negligible. Background was determined by placing approximately 7 mean free paths of absorbers on the holder. For most measurements the background was of the order of 5% of the detector counting rate with no absorbers present. The geometry was tested by comparing the attenuation of the 270 Mev. neutrons using the above geometry with the previous setup in which the detector was placed outside the concrete shielding in the collimated neutron beam. With the detector outside the shielding the background was negligible and the angular scattering correction less by a factor of two than in the present case.

To test the new geometry the length of copper absorber was increased by 3 inch steps to 12 inches and the resulting attenuation when corrected for background was linear as a function of absorber length when plotted on semi-logarithmic paper. If N_0 is the number of neutrons per second reaching the detector with no absorber present and N is the number when absorber of length ℓ is present

$$\frac{N-b}{N_0-b} = e^{-n\sigma_t \ell} \qquad A)$$

where b is the background counting rate when an absorber that absorbs essentially all the neutrons is placed in position, n is the number of nuclei per cubic centimeter, and σ_t is the total nuclear cross section. A value of $1.14 \pm .02 \times 10^{-24} cm^2$ was obtained with the detector as compared with the result outside the shielding of $1.15 \pm .02 \times 10^{-24} cm^2$ for the copper total cross section. Linear semi-log plots were obtained at other probe positions

to check the geometry. Most of the measurements were made with between one and two mean free paths of absorber present in order to obtain good statistics for a minimum time of cyclotron operation.

IV. ATTENUATOR MATERIALS

The metals used in the experiments were usually machined cylinders, 3 or 4 inches in diameter with negligible chemical impurities. Densities were obtained from measurements of the physical volumes with micrometer and vernier calipers and accurate weights of the cylinders.

The total cross section of hydrogen was measured using pentane-carbon differences. A brass cylindrical holder 48" long with 1/32" thick walls and bases held the pentane. An array of seven machined, 3" diameter graphite cylinders of mass per unit area equal to that of the carbon in the 48 inch length of pentane plus a 1/16" thick brass disc, and the pentane, were alternately used to attenuate the neutron beam. The decrease in the detector counting rate when the graphite was replaced by pentane is from the attenuation of the neutrons due to the hydrogen alone. Since only .3 to .4 mean free path of hydrogen is present (depending on the neutron energy) repeated cycles were made at a given probe setting to obtain good statistics. The percent statistical error of the cross section measurement is equal to the percent statistical error in counting divided by the number of mean free paths of hydrogen present. Short blank cycles were taken with an empty holder to obtain the carbon cross section.

The graphite and pentane were analyzed by the Pacific Chemical Laboratories for impurities, which were as follows:

MATERIAL	IMPURITIES	PERCENTAGE
Graphite	Silicon	0.052%
	Sulfur	0.067%
	Iron	0.011%
	Others	0.020%
Pentane	Sulfur	0.045%

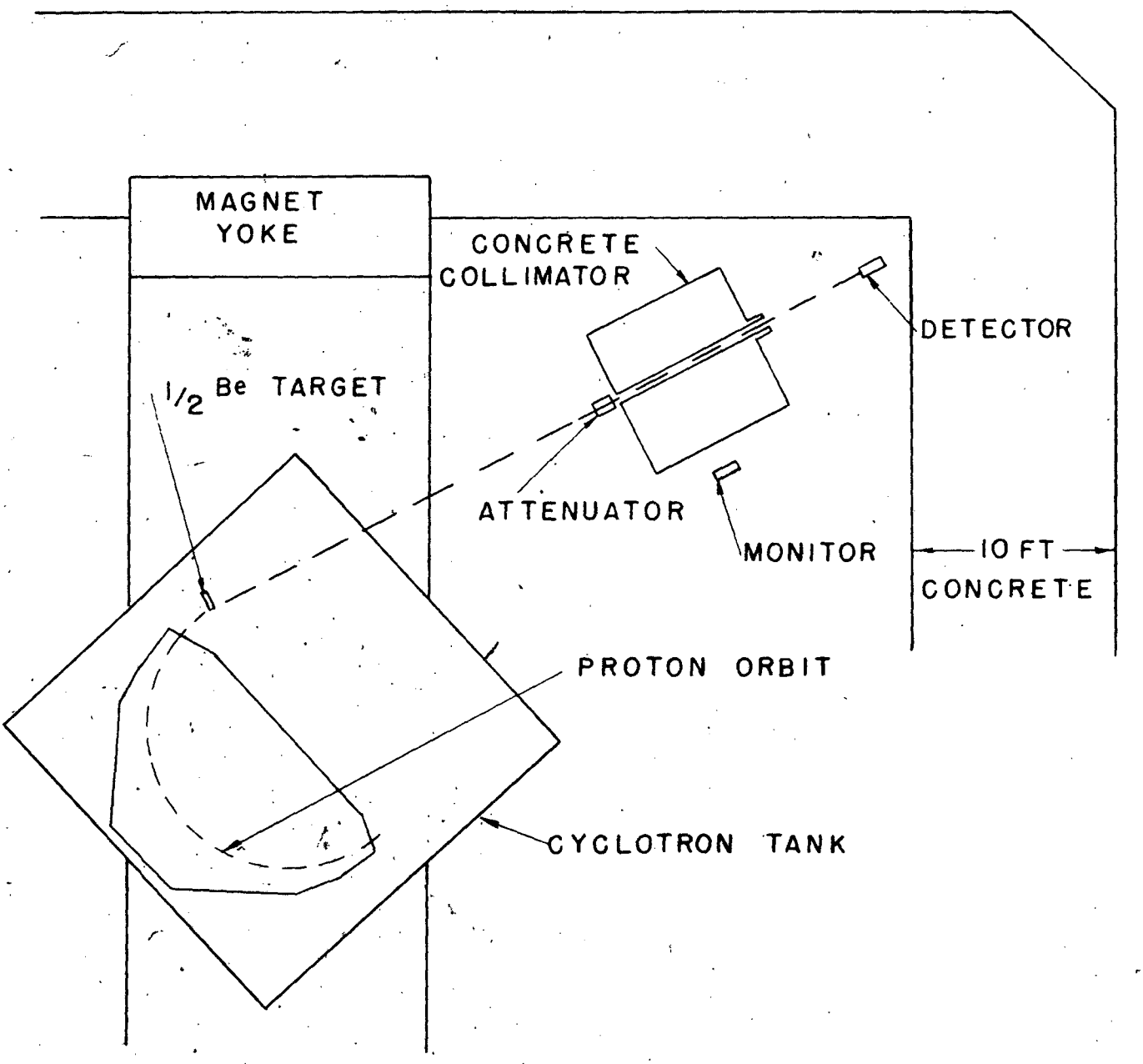

FIG. # 2

PLAN VIEW OF EXPERIMENTAL ARRANGEMENT

16000-1

V. SOURCES OF ERROR

Generally between one and two mean free paths of material were used in the measurements and the corrections for the diffraction scattering into the detector are small. Measurements of the ratio of inelastic to total cross sections for the 270 Mev. neutrons showed that the inelastic was at least half the total collision cross section. The present geometry was "good" to the extent that neutrons from the target could only be deflected 3/4 of a degree by the absorber at most and still enter the detector. The following nomenclature will be used for the diffraction scattering correction:

I_0 = no. of neutrons per steradian per sec. from beryllium target

r_1 = distance from target to absorber

r_2 = distance from absorber to detector

A_1 = effective cross sectional area of absorber for scattering neutrons into detector

A_2 = sensitive area of detector

N_s = no. of neutrons scattered per second by the absorber

N_d = no. of scattered neutrons entering the detector

N_0 = no. of undeviated neutrons entering detector with absorber in place

σ_t = total cross section

σ_e = cross section for elastic scattering

λ_e = mean free path for elastic scattering

λ_t = mean free path for elastic plus inelastic scattering (total M.F.P.)

ℓ = length of absorber

Ω = solid angle detector subtends at absorber = A_2/r_2^2

n = no. of nuclei per cm^2

The probability of a neutron being elastically scattered p times as it traverses a length ℓ of material is:

(1) $P_p = (\ell/\lambda_e)^p \frac{1}{p!} e^{-\ell/\lambda_t}$ from Poisson's formula.

Assuming that a neutron singly scattered is always deflected through an angle α, where α is a small angle, a neutron scattered p times will be at an angle $\alpha p^{1/2}$ with respect to its initial direction (from the random walk problem). If the detector has a maximum angle of reception from the absorber, θ, the initial maximum angle of scattering must be $\frac{\theta}{p^{1/2}}$ for neutrons scattered p times to be accepted. The solid angle these p fold scattered neutrons can enter after their initial deflection is equal to .

The probability of a neutron being scattered p times and entering the detector at angle θ is:

(2) $$P_{\theta d} = \frac{1}{p!}(\ell/\lambda_e)^p \frac{e^{-\ell/\lambda_t}}{\sigma_e} \frac{d\sigma_e(\theta/p^{1/2})}{d\omega} \frac{2\pi \sin\theta\, d\theta}{p}$$

The number of scattered neutrons entering the detector per second between angles θ and $\theta + d\theta$ is:

$$N_{\theta d} = I_0 \frac{A_1}{r_1^2}\left[\sum_{p=1}^{\infty} \frac{1}{p!\,p}(\ell/\lambda_e)^p \frac{d\sigma_e(\theta/p^{1/2})}{d\omega}\right]\frac{e^{-\ell/\lambda_t}}{\sigma_e} 2\pi \sin\theta\, d\theta$$

Since the maximum angle of acceptance is only 3/4 of a degree at the detector, the differential scattering cross section is practically constant over this small angular range and may be replaced by $\frac{d\sigma_e(0°)}{d\omega}$. The solid angle, $2\pi \sin\theta\, d\theta$, integrates to A_2/r_2^2.

Finally:

(3) $$N_d = I_0 \frac{A_1}{r_1^2} \frac{A_2}{r_2^2} \frac{d\sigma_e(0°)}{d\omega} \frac{e^{-\ell/\lambda_t}}{\sigma_e} \sum_{p=1}^{\infty} \frac{1}{p!\,p}(\ell/\lambda_e)^p$$

But

$$N_0 = I_0 \frac{A_2}{(r_1 + r_2)^2} e^{-\ell/\lambda_t}$$

Therefore (4)

$$\frac{N_d}{N_0} = \frac{A_1}{\sigma_e} \frac{d\sigma_e(0°)}{d\omega}\left[\frac{1}{r_1} + \frac{1}{r_2}\right]^2 \sum_{p=1}^{\infty} \frac{1}{p!\,p}(\ell/\lambda_e)^p$$

Writing the summed terms in expanded form

$$\frac{N_d}{N_0} = \frac{A_1}{\sigma_e}\frac{d\sigma_e(0^\circ)}{d\omega}\left[\frac{1}{r_1}+\frac{1}{r_2}\right]^2\left[\frac{\ell}{\lambda_e}+\frac{1}{2!2}\left(\frac{\ell}{\lambda_e}\right)^2+\frac{1}{3!3}\left(\frac{\ell}{\lambda_e}\right)^3+\cdots\right]$$

since $\lambda_e = \frac{1}{n\sigma_e}$

$$= \frac{A_1}{\sigma_e}\frac{d\sigma_e(0^\circ)}{d\omega}\left[\frac{1}{r_1}+\frac{1}{r_2}\right]^2\left[\ell n\sigma_e+\frac{1}{2!2}\ell^2 n^2\sigma_e^2\right]$$

For the accurate measurements of cross sections ℓ was always less than λ_e, so the first term in the expansion dominates the rest. The 270 Mev. experiments showed that $\sigma_e \lesssim 0.5\sigma_t$. In the corrections we will use $\sigma_e = .5\sigma_t$, which will give an upper limit to the correction. The above treatment is essentially the same as that of McMillan.

The differential scattering cross sections were estimated from the transparent model. At 190 and 270 Mev. they are[16]:

TABLE 1

Element	$\frac{d\sigma_e(0^\circ)}{d\omega}$ (190 Mev.)	$\frac{d\sigma_e(0^\circ)}{d\omega}$ (270 Mev.)
Cu	11.6 $\frac{\text{barns}}{\text{steradian}}$	15.4 $\frac{\text{barns}}{\text{steradian}}$
Sn	27.5	37.2
Pb	60.5	81.5
U	74.0	100.0

For the lead and uranium cross sections the correction amounted to about 1% at 190 Mev. with the geometry employed, and dropped to about half this value for copper. Since the statistical errors in the cross section values are about three or four times the correction, an uncertainty of 50% in the correction is tolerable. The assumptions made in the calculations are presumably within this figure.

A background of scattered neutrons from the tank wall comprising 10 to 20% of the neutron flux from the target may be present in the region

where the absorbers are placed. The angular acceptance of the detector is such that most of these neutrons cannot enter the detector unless they are scattered by the absorbers. Since elastic scattering maximizes in the forward direction the above considerations indicate that the error introduced by this effect will be negligible.

VI. RESULTS

The data obtained are given in Table 2. Copper, tin, lead, and uranium have small diffraction scattering corrections incorporated into their cross section values. The variations of the cross sections with energy are shown in graphical form for carbon, aluminum, copper, and lead (Figure 4). The hydrogen cross section is illustrated in Figures 5 and 6. The results of the previously quoted sources are given as well as the 42 Mev. cross sections of Hildebrand and Leith[17] (to be published). The errors given are the statistical fluctuations from counting alone expressed in standard deviations.

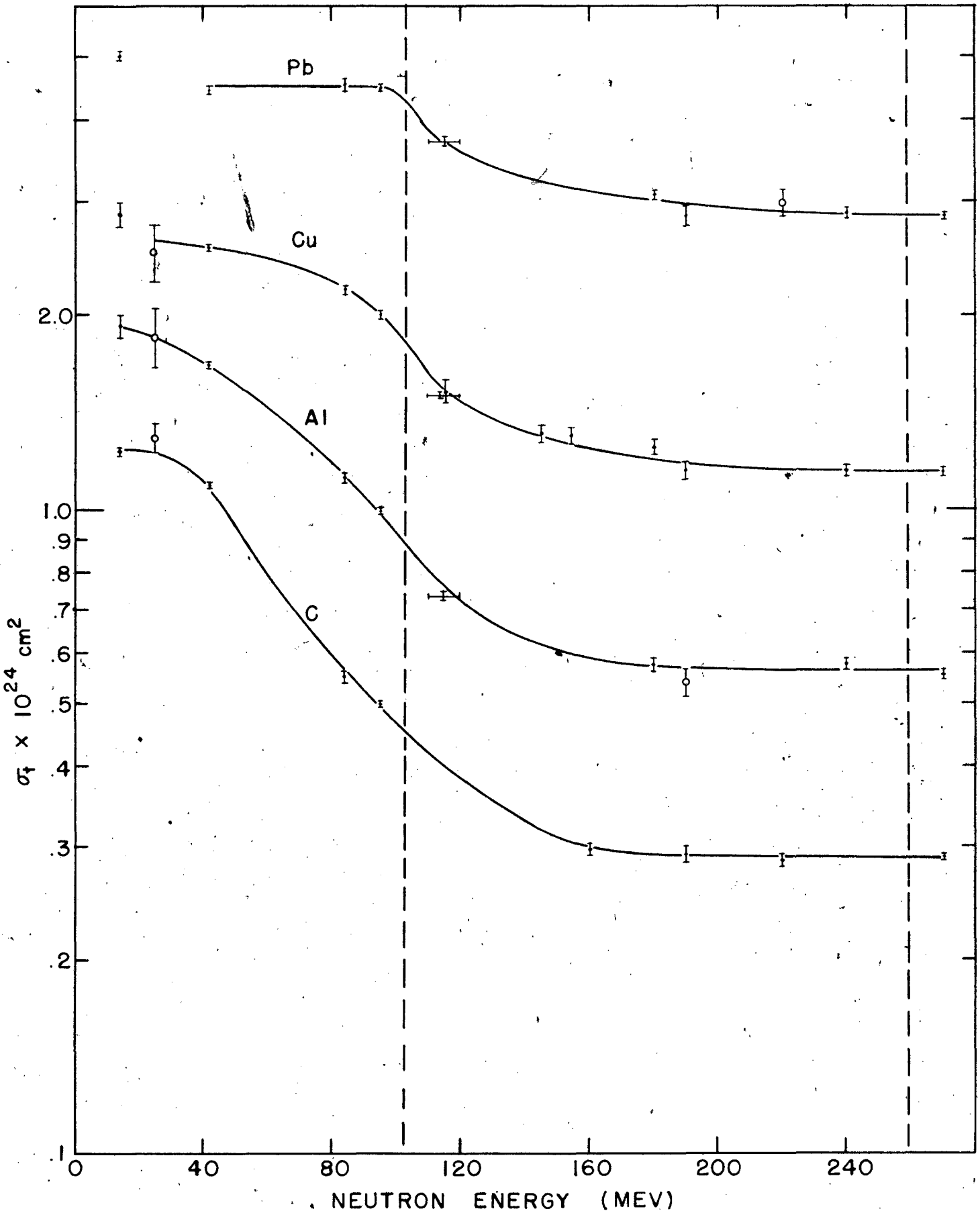

TOTAL CROSS SECTIONS FOR HIGH ENERGY NEUTRONS

FIG. # 3

16001-1

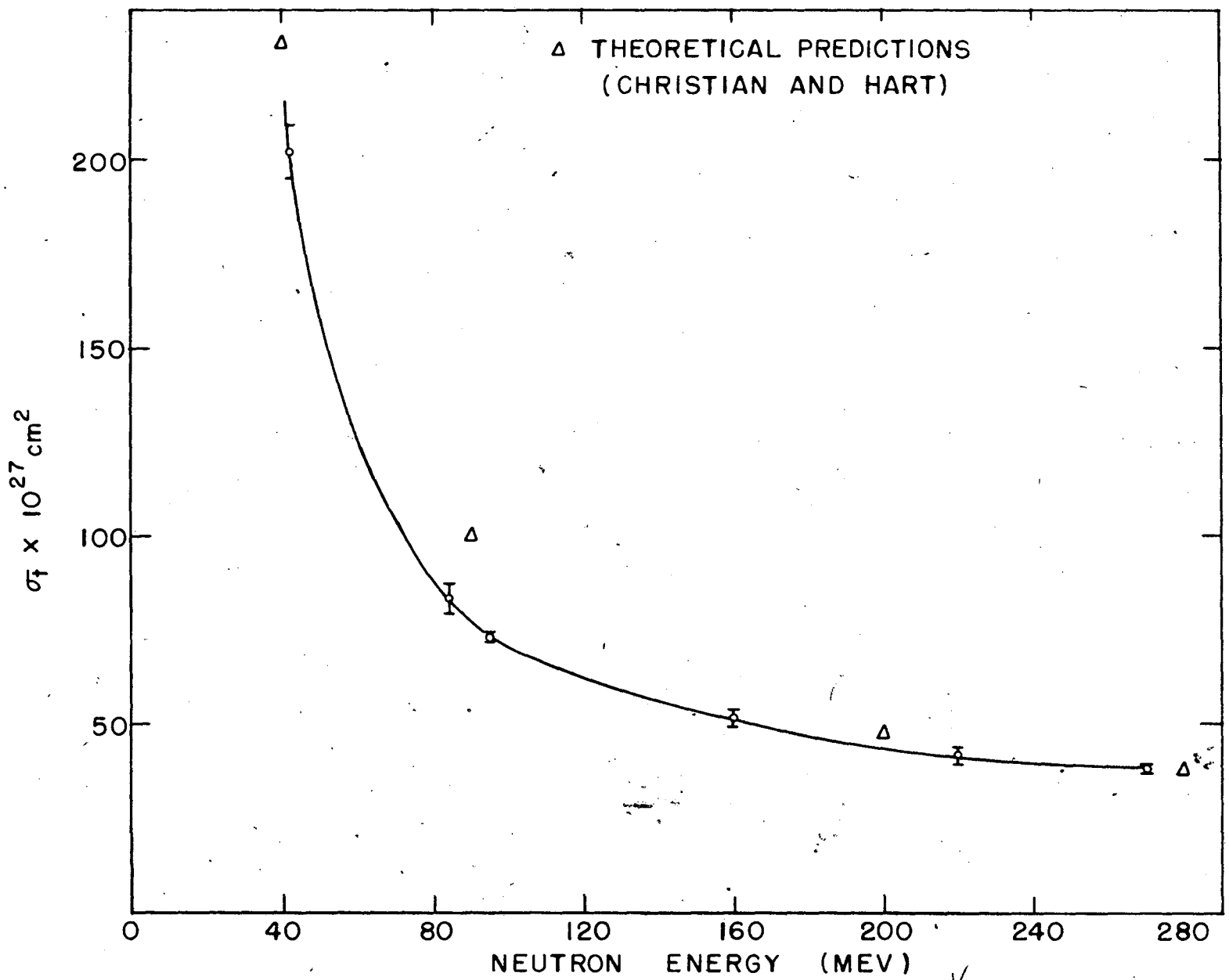

HYDROGEN TOTAL CROSS-SECTION AS FUNCTION OF NEUTRON ENERGY

FIG. 4

16002-

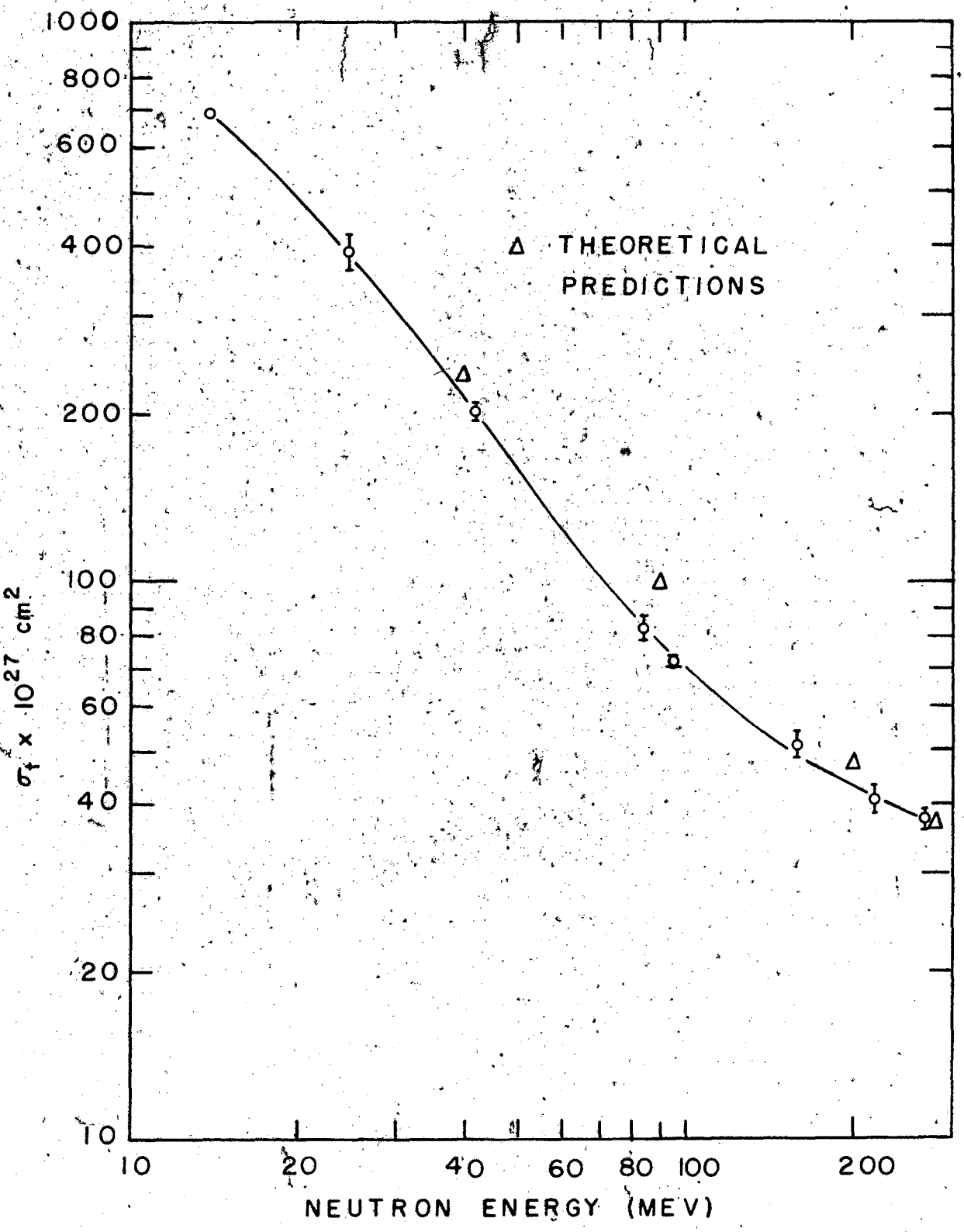

FIG. 6

HYDROGEN TOTAL CROSS SECTION AS FUNCTION OF NEUTRON ENERGY.

TABLE 2

TOTAL CROSS SECTIONS OF NUCLEI FOR HIGH ENERGY NEUTRONS MEASURED WITH BISMUTH FISSION CHAMBERS

Proton Energy	Target	Estimated Neutron Energy	Element	$\sigma_t \times 10^{24}$ cm^2
310 Mev.	0.5" Be	240 Mev.	Al	0.576 ± .012
			Cu	1.15 ± .02
			Pb	2.88 ± .05
290 Mev.	0.5" Be	220 Mev.	H	1) 0.0410 ± .0041
				2) 0.0410 ± .0029
				0.041 ± .0024 (ave.)
			C	1) 0.288 ± .10
				2) 0.283 ± .08
				0.285 ± .06 (ave.)
			Al	0.576 ± .021
			Cu	1.15 ± .035
			Pb	2.99 ± .14
270 Mev.	2" Be	190 Mev.	C	0.291 ± .009
			Al	0.540 ± .028
			Cu	1.15 ± .04
			Sn	1.90 ± .07
			Pb	2.85 ± .10
			U	3.28 ± .13
250 Mev.	0.5" Be	180 Mev.	Al	0.575 ± .013
			Cu	1.25 ± .03
			Pb	3.06 ± .06
230 Mev.	0.5" Be	160 Mev.	H	1) 0.0548 ± .0060
				2) 0.0504 ± .0029
				0.0512 ± .0026 (ave.)
			C	1) 0.298 ± .012
				2) 0.295 ± .0075
				0.296 ± .006 (ave.)
225 Mev.	2" Be	145 Mev.	Cu	1.31 ± .04
	0.5" Be	155 Mev.	Cu	1.30 ± .04
185 Mev.	0.5" Be	115 Mev.	Cu	1.52 ± .06
180-190*	0.5" Be	110-120 Mev.	Al	0.733 ± .012
			Cu	1.49 ± .02
			Pb	3.71 ± .06

*Probe position not accurately known

TABLE 3

TOTAL CROSS SECTIONS FOR 95 AND 270 MEV. NEUTRONS MEASURED PREVIOUSLY WITH BISMUTH FISSION CHAMBERS

Element	σ_t(95 Mev.) x 10^{24} cm^2	σ_t(270 Mev.) x 10^{24} cm^2
Hydrogen	0.073 ± .0015	0.038 ± .0015
Carbon	0.498 ± .003	0.288 ± .003
Aluminum	0.993 ± .011	0.555 ± .008
Copper	2.00 ± .02	1.15 ± .02
Lead	4.48 ± .03	2.84 ± .03

VII. DISCUSSION OF RESULTS

Carbon, aluminum, copper and lead all exhibit plateaus in their total cross section values from about 180 Mev. to 270 Mev. mean neutron energy, as Figure 4 indicates. The neutron energy distribution detected by the fission chambers is rather broad for the measurements undertaken and the resulting cross sections may not correspond exactly to the true cross section at the mean detected energy of the unattenuated distribution. If the detected energy distribution is given by f(E) where f(E) is normalized so that $\int_{E_{min.}}^{E_{max.}} f(E)dE = 1$ the measured value of the cross section is from A)

$$n\ell\sigma_m = \ln\frac{N_0-b}{N-b} = -\ln\int_{E_{min.}}^{E_{max.}} f(E)e^{-n\sigma_t(E)\ell}dE$$

or $$\sigma_m = \frac{-1}{n\ell}\ln\int_{E_{min.}}^{E_{max.}} f(E)e^{-n\sigma_t(E)\ell}dE \qquad \text{B)}$$

If σ_m is examined for the energy intervals where measurements were made the following statements may be made for the four nuclei above:

(1) For mean energies of 240 Mev. and above the variation of $\sigma_t(E)$ over the distribution is slight and σ_m agrees with $\sigma(\bar{E})$ at the mean energy

$$\bar{E} = \int_{E_{min.}}^{E_{max.}} E\,f(E)\,dE.$$

(2) As the mean energy of the distribution is lowered to 160 Mev, $\sigma_t(E)$ begins to increase from the plateau value on the low energy side of the distribution and the measured value σ_m will be higher than $\sigma(\bar{E})$.

A sample calculation was made for a bell shaped neutron energy distribution with a 60 Mev. width at half maximum and an absorber 1.5 mean free paths in length at the mean neutron energy. For a cross section decreasing about as carbon does, σ_m at 160 Mev. could be about 5% higher than the true σ(160 Mev).

In general the broad distribution tends to round off the shape of the curves. The plateaus are probably slightly flatter and longer in extent than shown.

A measurement of the energy distribution of the neutrons resulting from the bombardment of a 0.5" Be target with 180 Mev. protons would enable one to determine the energy assignments of cross sections measured between 100 and 160 Mev. to a better extent than is possible now.

The region where the cross sections tend to level off is near the theoretical threshold for π meson production with neutrons which is of the order of 150 Mev. from conservation laws[18]. The transparency of the nuclei to neutrons apparently reaches a limit near 200 Mev. Since the change in the propagation vector, k_1, in the theory of the transparent nucleus, had to be taken equal to zero in order to obtain even an approximate fit of the theory to the data at 270 Mev. the cross sections were presumably a function of the absorption coefficient K alone. At 270 Mev. the theory predicted higher cross-section values for the heavy nuclei than were measured and a fit could be obtained by assuming K decreased with atomic number. At 90 Mev. the agreement was not very sensitive to K, as mentioned earlier, and a constant value gave satisfactory results. Since the ratio of neutrons to protons in nuclei increases with atomic number K would not be constant if the n-n cross section were smaller than the n-p cross section for the neutron traversing nuclear matter. Since σ_t, σ_e, and σ_i are all functions of K alone, measurements of the inelastic cross sections for a few of the nuclei with a detector having a neutron energy cutoff near 270 Mev. are needed to settle the problem conclusively.

The total n-p cross section variation with energy is given in Figures 5 and 6. The theoretical predictions of Christian and Hart[19] for a Yukawa potential with tensor interaction are shown also. Experimentally the cross section deviates more markedly from an 1/E variation than the theoretical dependence does.

Measurements of the differential scattering and total n-p cross sections in the region above 300 Mev. may provide information which will shed light on proposed models of nucleon interaction, such as the recently discussed "hard core" model. When the neutron energy reaches the region where mesons begin to be produced, implying that inelastic collisions between nucleons occur, it may be expected that a change in the characteristics of the scattering pattern would be observed. In the neutron bombardment of hydrogen the threshold for π meson production is about 295 Mev., if the π meson is assumed to possess 276 electron masses.

ACKNOWLEDGEMENTS

The author wishes to express his thanks to members of the committee and in particular to Dr. B. J. Moyer who suggested the investigation and whose continued interest and advice were invaluable. Discussions of the results with Professor R. Serber and Messrs. Fernbach and Christian were enlightening. Thanks must be expressed also to Mr. A. Redmond, who assisted in most of the experimental work, especially in the arduous task of aligning the collimator and to the cyclotron crew for their cooperation.

REFERENCES

(1) Amaldi, Bocciarelli, Cacciapuoti, and Trabachi, Nuovo Cimento 3, 203 (1946).

(2) R. Sherr, Phys. Rev. 68, 240, (1945).

(3) V. Weisskopf, Los Alamos Report 24.

(4a) A. Helmholz, E. McMillan, and D. Sewell, Phys. Rev. 72, 1003 (1947).

(4b) R. Serber, Phys. Rev. 72, 1008, (1947).

(5) L. Cook, E. McMillan, J. Peterson, and D. Sewell, Phys. Rev. 75, 7 (1949).

(6) J. DeJuren and N. Knable, Phys. Rev. 77, 606, (1950).

(7) S. Fernbach, R. Serber, and T. B. Taylor, Phys. Rev. 75, 1352, (1949).

(8) R. Fox, C. Leith, L. Wouters, and K. McKenzie (To be published, Phys. Rev.).

(9) J. DeJuren (To be published, Phys. Rev.).

(10) C. Wiegand, Rev. Sci. Instruments, 19, 790, (1948).

(11) J. Cladis and J. Hadley (Private communication).

(12) Fox, Leith, and Wouters (Private communication).

(13) Kelly, Wiegand, and Segre (To be published).

(14) L. Baumhoff (Private communication).

(15) R. Fox and L. Wouters (Private communication).

(16) S. Fernbach (Private communication).

(17) R. Hildebrand and C. Leith (To be published, Phys. Rev.).

(18) W. Barkas, Phys. Rev. 75, 1109, (1949).

(19) R. Christian and E. Hart, Phys. Rev. 77, 441, (1950).